

# A basic study on incidence directivity analysis using multipole and local expansions

Yosuke Yasuda<sup>1,\*</sup>, Takayuki Masumoto<sup>2</sup>, Naohisa Inoue<sup>3</sup> and Tetsuya Sakuma<sup>4</sup>

<sup>1</sup>Kanagawa University, 3-27-1 Rokkakubashi, Kanagawa-ku, Yokohama, 221-8686 Japan

<sup>2</sup>Cybernet Systems Co., Ltd., Fujisoft Bldg. 3 Kanda-neribeicho, Chiyoda-ku, Tokyo, 101-0022 Japan

<sup>3</sup>Maebashi Institute of Technology, 460-1 Kamisadori, Maebashi, 371-0816 Japan

<sup>4</sup>The University of Tokyo, 7-3-1 Hongo, Bunkyo-ku, Tokyo, 113-8656 Japan

(Received 10 August 2021, Accepted for publication 8 September 2021)

**Keywords:** Incidence directivity, Plane wave expansion, Multipole expansion, Local expansion, FMBEM

## 1. Introduction

The directivity of incident sound (incidence directivity) is important when evaluating the diffuseness of rooms and the effectiveness of sound diffusers/absorbers. There is an approach to evaluate incidence directivity using the plane wave expansion (angular spectrum [1]), and recently, this approach has been applied to the evaluation of isotropy in reverberation rooms [2] and the evaluation of oblique incidence sound absorption coefficients [3], for example. On the other hand, to calculate a reliable incidence directivity using the plane wave expansion, it is essential to clarify various types of numerical error and the relationship between the calculated incidence directivity and the corresponding sound-receiving region.

The plane wave expansion also appears in the fast multipole boundary element method (FMBEM), which is well known as a highly efficient wave-based numerical method. By combining the representation of incidence directivity using the plane wave expansion and numerical analysis of sound fields by FMBEM, the incidence directivity for various regions in space can be calculated with high efficiency. For sound radiation/reflection directivity, a fast calculation method using FMBEM has been already reported [4].

In this work, considering an application to an efficient calculation of incidence directivity based on FMBEM, a basic study with a point source and receiving regions is conducted. We investigate the numerical errors caused by multipole and local expansions, which are the basis of FMBEM, and discuss the relationship between the incidence directivity and the receiving region.

## 2. Calculation of incidence directivity using multipole and local expansions

We assume a steady-state sound field with a point source, which is represented by the fundamental solution of the Helmholtz equation, and describe the relationship among the plane wave expansion, multipole and local expansions, incidence directivity, and receiving region.

### 2.1. Plane wave expansion of fundamental solution

Consider point source  $q$ , receiving point  $p$ , multipole

expansion point  $M$ , and local expansion point  $L$ , which satisfy  $r_{pL} + r_{Mq} < r_{LM}$ . In a steady-state sound field, contribution at receiving point  $p$  from point source  $q$  is represented in the form of plane wave expansion of the fundamental solution as follows:

$$h_0^{(1)}(kr_{pq}) = \frac{e^{jkr_{pq}}}{jkr_{pq}} = \frac{1}{4\pi} \oint E(\hat{\mathbf{k}}, \mathbf{r}_{pL}) s(\hat{\mathbf{k}}) d\hat{\mathbf{k}}, \quad (1)$$

$$E(\hat{\mathbf{k}}, \mathbf{r}_{pL}) = \exp(j\mathbf{k} \cdot \mathbf{r}_{pL}), \quad (2)$$

$$s(\hat{\mathbf{k}}) = T(\hat{\mathbf{k}}, \mathbf{r}_{LM}) E(\hat{\mathbf{k}}, \mathbf{r}_{Mq}), \quad (3)$$

$$T(\hat{\mathbf{k}}, \mathbf{r}_{LM}) = \sum_{l=0}^{N_p-1} j^l (2l+1) h_l^{(1)}(kr_{LM}) P_l(\hat{\mathbf{k}} \cdot \hat{\mathbf{r}}_{LM}), \quad (4)$$

where  $\mathbf{r}_{pq} = \mathbf{r}_p - \mathbf{r}_q$ ,  $\mathbf{k}$  is the wavenumber vector,  $k = |\mathbf{k}|$ ,  $\hat{\mathbf{k}} = \mathbf{k}/k$ ,  $h_l^{(1)}$  are spherical Hankel functions of the first kind,  $P_l$  are Legendre polynomials,  $N_p$  is the truncation number for the infinite sum, and  $\oint d\hat{\mathbf{k}}$  represents the integral over the unit sphere. This form, including a series expansion  $T$  represented by Eq. (4), is derived from the multipole expansion of the fundamental solution [5].

### 2.2. Incidence directivity and receiving region

Equation (1) represents a plane wave expansion at local expansion point  $L$ , and  $E(\hat{\mathbf{k}}, \mathbf{r}_{pL})$  represents a plane wave with a unit amplitude coming from the direction of  $\hat{\mathbf{k}}$ . Therefore, the amplitude of the plane wave coming from the direction of  $\hat{\mathbf{k}}$  to point  $p$  is written as  $|E(\hat{\mathbf{k}}, \mathbf{r}_{pL}) s(\hat{\mathbf{k}})| = |s(\hat{\mathbf{k}})|$ . This is the incidence directivity at point  $p$ . If one can set point  $p$  freely within the region where  $r_{pL} < r_{LM} - r_{Mq}$  is satisfied,  $|s(\hat{\mathbf{k}})|$  can be regarded as the incidence directivity of the receiving region in a sphere of radius  $r_{LM} - r_{Mq}$  centered at point  $L$ . However, the receiving region is numerically more limited because of the truncation of the infinite sum in Eq. (4).

### 2.3. Plane wave expansion and local expansion

#### 2.3.1. Local expansion of fundamental solution

The fundamental solution is represented by a local expansion at expansion point  $L$  as follows:

$$h_0^{(1)}(kr_{pq}) = \sum_{n=0}^{N_L-1} \sum_{m=-n}^n L_n^m R_n^m(\mathbf{r}_{pL}), \quad (5)$$

$$L_n^m = 4\pi h_n^{(1)}(kr_{qL}) Y_n^m(\hat{\mathbf{r}}_{qL}) = 4\pi S_n^m(\mathbf{r}_{qL}), \quad (6)$$

$$S_n^m(\mathbf{r}) = h_n^{(1)}(kr) Y_n^m(\hat{\mathbf{r}}), \quad R_n^m(\mathbf{r}) = j_n(kr) Y_n^m(\hat{\mathbf{r}}), \quad (7)$$

where  $\mathbf{r} = (r, \theta, \varphi)$ ,  $\hat{\mathbf{r}} = \mathbf{r}/r = (\theta, \varphi)$ ,  $L_n^m$  are local expansion

\*e-mail: yyasuda@kanagawa-u.ac.jp

[doi:10.1250/ast.43.77]

coefficients,  $j_n$  are spherical Bessel functions,  $Y_n^m$  are spherical harmonics, and  $N_L$  is the truncation number for the local expansion.

### 2.3.2. Conversion of expansion coefficients

The plane wave expansion coefficients (angular spectrum)  $s$  and the local expansion coefficients  $L_n^m$  can be converted to each other by the spherical harmonic transform and its inverse:

$$s(\hat{\mathbf{k}}) = \sum_{n=0}^{N_L-1} \sum_{m=-n}^n j^{-n} L_n^m Y_n^m(\hat{\mathbf{k}}), \quad (8)$$

$$L_n^m = j^n \oint s(\hat{\mathbf{k}}) Y_n^{-m}(\hat{\mathbf{k}}) d\hat{\mathbf{k}}. \quad (9)$$

## 3. Numerical experiments

### 3.1. Setup

**Outline** Figure 1 shows two analysis cases. The positions of source point  $q$  and expansion point  $L$  are fixed in the two cases. Expansion point  $M$  and source point  $q$  coincide in Case A, but not in Case B. The distance between expansion points  $L$  and  $M$  is the same in the two cases. By the calculation procedures shown below, the incidence directivity  $|s|$  of the receiving region including point  $L$  is calculated. The value  $h_0^{(1)}$  is also calculated at receiving point  $p$  on the plane  $z = 0$ , which includes points  $q$ ,  $L$ , and  $M$ , and compared with the theoretical value  $h_{0,th}^{(1)} = e^{jkr_{pq}} / (jkr_{pq})$ . In both cases, the effect is investigated by changing the truncation number for the infinite sum,  $N_p$  or  $N_L$ .

**Calculation of  $s$  and  $h_0^{(1)}$**  The values of  $s$  are calculated using Eq. (3), where expansion  $T$  is up to  $l = N_p - 1$ . The

values of  $h_0^{(1)}$  are also calculated using Eq. (1) with  $s$ . For comparison, the values of  $L_n^m$  up to  $n = N_L - 1$  are calculated using Eq. (6) and those of  $h_0^{(1)}$  are calculated using Eq. (5) with  $L_n^m$  based on the local expansion. The values of  $s$  are converted from  $L_n^m$  using Eq. (8). For the local expansions, source point  $q$  and expansion point  $L$  are assumed, but expansion point  $M$  is not.

**The integral over the unit sphere** Regarding the integral over the unit sphere in Eqs. (1) and (9), Gauss–Legendre quadrature (the number of quadrature points  $N_k$ ) in the  $\theta$  direction and trapezoidal quadrature (the number of quadrature points  $2N_k$ ) in the  $\varphi$  direction are employed, and  $N_k$  is fixed to  $N_p - 1$ .

### 3.2. Results and discussion

Figure 2 shows incidence directivities  $|s|$ . Figures 3 to 5 show the spatial distributions of  $h_0^{(1)}$  on the receiving plane  $z = 0$ , together with the distributions of the relative error  $\varepsilon_h$  calculated using the following formula:

$$\varepsilon_h = \frac{|h_{0,approx}^{(1)} - h_{0,th}^{(1)}|}{|h_{0,th}^{(1)}|}, \quad (10)$$

where  $h_{0,approx}^{(1)}$  denotes  $h_0^{(1)}$  calculated through the above-mentioned procedures. In all cases,  $kr_{qL} = 30$ .

#### 3.2.1. Calculation based on local expansion

Firstly, as a reference, the results calculated based on the local expansion are presented.

**Incidence directivity (Fig. 2)** As mentioned above,  $|s|$  is regarded as the incidence directivity for a certain receiving region centered at point  $L$ . From Figs. 2 and 3,  $|s|$  can be interpreted as the directivity for the region where  $h_0^{(1)}$  are calculated with high accuracy, which depends on  $N_L$  (hereafter, we call this region the high-accuracy region). The directivities point toward the source when  $N_L \leq kr_{qL}$ , whereas strong directivities on the opposite side of the source are observed when  $N_L$  is larger ( $N_L \geq 2kr_{qL}$ ). This result deviates from the general tendency of directivity. The same was true for other dimensionless wavenumbers ( $kr_{qL} = 60, 120$ ). This is because a wide region of the sound field, including the vicinity of the source, is expanded by plane waves. Mathematically, this corresponds to the divergence of  $h_n^{(1)}$  in  $L_n^m$ .

**High-accuracy region (Fig. 3)** As the truncation number  $N_L$  for the infinite sum increases, the high-accuracy region spreads spherically around point  $L$  (0,0,0). In this figure,

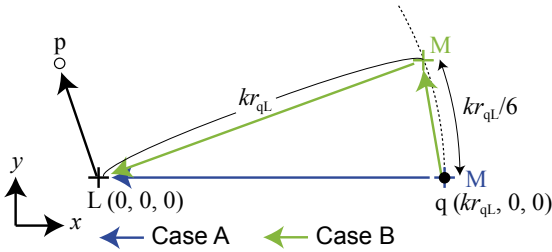


**Fig. 1** Analysis cases: Case A, where points  $M$  and  $q$  coincide, and Case B, where  $M$  and  $q$  do not coincide.

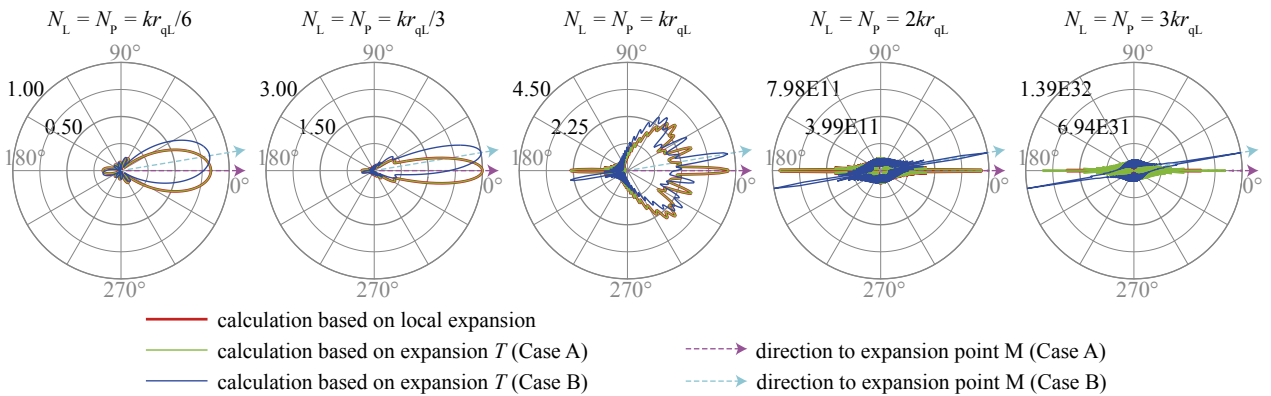


**Fig. 2** Incidence directivities  $|s|$  ( $kr_{qL} = 30$ ).

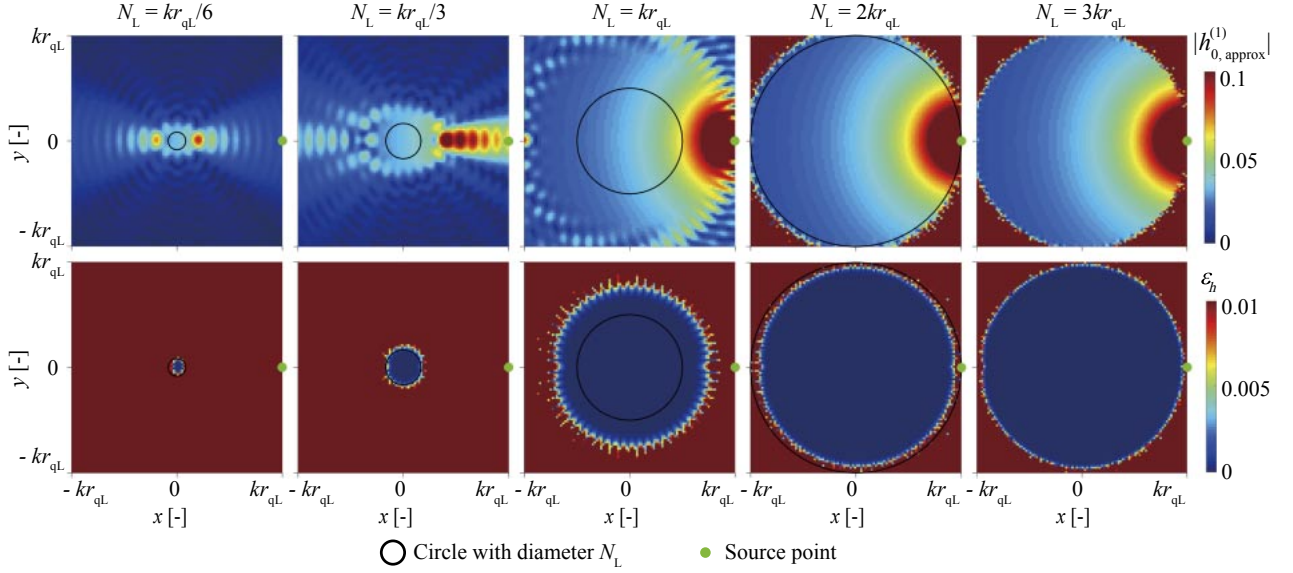


**Fig. 3**  $h_{0,approx}^{(1)}$  calculated using Eq. (5) and relative error  $\varepsilon_h$  ( $kr_{qL} = 30$ ).

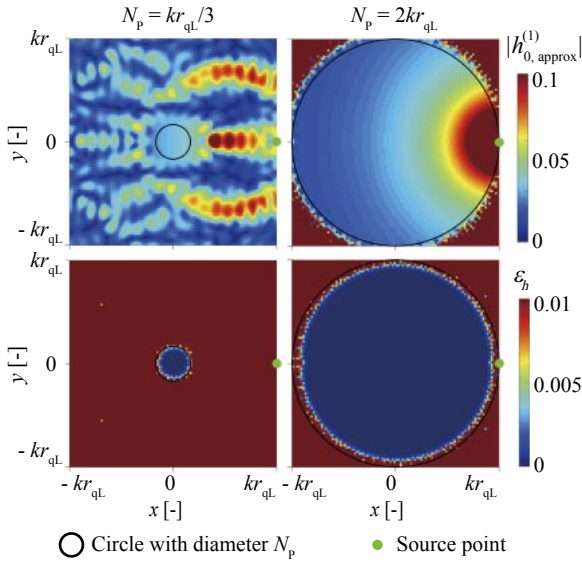


**Fig. 4**  $h_{0,approx}^{(1)}$  calculated using Eq. (1) and relative error  $\varepsilon_h$  for Case A ( $kr_{qL} = 30$ ). Values diverged when  $N_p = 3kr_{qL}$ .

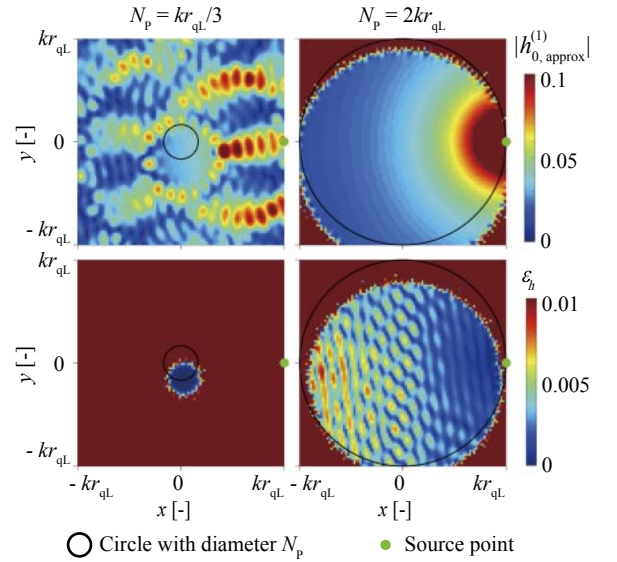


**Fig. 5**  $h_{0,approx}^{(1)}$  calculated using Eq. (1) and relative error  $\varepsilon_h$  for Case B ( $kr_{qL} = 30$ ). Values diverged when  $N_p = 3kr_{qL}$ .

circles with a diameter of  $N_L$  centered on point L are also shown, and these circles roughly correspond to the high-accuracy regions until the region reaches source point q ( $N_L \leq 2kr_{qL}$ ). In other words, when the local expansion is used, the calculation accuracy is maintained even if the expansion includes the high-order components. This is because the spherical Hankel function  $h_n^{(1)}$  diverges as  $n$  increases, whereas the spherical Bessel function  $j_n$  converges to 0. Consequently, the local expansion Eq. (5) containing  $j_n h_n^{(1)}$  converges well.

### 3.2.2. Calculation based on expansion $T$ (Case A)

**Incidence directivity (Fig. 2)** Only the result with  $N_p = 3kr_{qL}$  is different from the local expansion result. This is also

due to the divergence of  $h_n^{(1)}$ , but its effect appears differently from that in the case of the local expansion. This is probably caused by the difference in the high-order components around the truncation number for the infinite sum, between  $s$  directly calculated using Eq. (3) and  $s$  converted from  $L_n^m$  using Eq. (8).

**High-accuracy region (Fig. 4)** Being different from the local expansion case, the values diverged and there was no highly accurate region when  $N_p = 3kr_{qL}$  (results are omitted). This is because expansion  $T$  (Eq. (4)) does not include any converging functions that cancel the divergence of  $h_n^{(1)}$ . As is well known, for Eq. (1) to be effective, there must be no high-order components of the infinite sum in Eq. (4) [6]. In

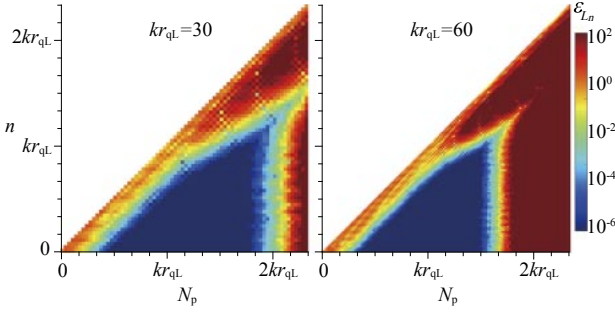


Fig. 6 Relationship between  $N_p$  and  $\varepsilon_{L_n}$  for Case B.

the cases of larger dimensionless wavenumbers ( $kr_{qL} = 60, 120$ ), the values diverged even with  $N_p = 2kr_{qL}$ . This suggests that it is necessary to satisfy  $N_p \lesssim kr_{qL}$  in general.

### 3.2.3. Calculation based on expansion $T$ (Case B)

**Incidence directivity (Fig. 2)** The directivities  $|s|$  point toward expansion point M, not toward source point q. This is reasonable because  $|s| = |T|$  (Eq. (3)) and  $T$  depends only on  $\hat{k}$  and  $\mathbf{r}_{LM}$ , not on the position of point q (Eq. (4)). That is, when calculated directly using Eq. (3), the directivity  $|s|$  points not toward the real sound source, but toward the converted multipole sound source.

**High-accuracy region (Fig. 5)** The high-accuracy regions move slightly downward in accordance with the position of expansion point M.

### 3.2.4. Calculation accuracy of $L_n^m$ converted from $s$

In Case B, we converted the values of  $s$  with the truncation number  $N_p$  to the values of  $L_n^m$  up to  $N_L = N_p$  using Eq. (9). Next, we calculated the relative error of these values with respect to the true values of  $L_n^m$  for each  $n$ -th order component using the following formula:

$$\varepsilon_{L_n} = \frac{\left| \sum_{m=-n}^n L_{n,\text{approx}}^m - \sum_{m=-n}^n L_{n,\text{th}}^m \right|}{\left| \sum_{m=-n}^n L_{n,\text{th}}^m \right|}, \quad (11)$$

where  $L_{n,\text{approx}}^m$  are  $L_n^m$  converted from  $s$  and  $L_{n,\text{th}}^m$  are  $L_n^m$  directly calculated using Eq. (6).

Figure 6 shows the relationship between  $N_p$  and  $\varepsilon_{L_n}$ . In the area of large  $N_p$ , the error is large regardless of order  $n$  because of the divergence of  $h_n^{(1)}$  in Eq. (4). On the other hand, in the area of small  $N_p$ , the error is extremely small with low order  $n$ . We have confirmed that if  $s$  is reconstructed using only these low-order components, a highly accurate incidence directivity that points toward the actual source

can be calculated, like the calculation based on local expansion [7].

## 4. Conclusions

Our conclusions are summarized below.

- The plane wave expansion coefficients can be interpreted as the incidence directivity for a certain finite region (high-accuracy region) including the expansion point.
- The high-accuracy region and the corresponding incidence directivity change depending on the truncation number for the expansion. In other words, the incidence directivity for a region of the desired size can be calculated by controlling the truncation number for the expansion.
- The high-accuracy region roughly corresponds to the interior region of a sphere centered at the expansion point with a diameter of approximately the truncation number for the expansion.
- When directly calculating the plane wave expansion coefficients using expansion  $T$ , it is necessary to convert them to the local expansion coefficients and then reconvert them to the plane wave expansion coefficients using only the low-order components of the local expansion coefficients.

## References

- [1] E. G. Williams, *Fourier Acoustics: Sound Radiation and Near-Field Acoustical Holography* (Academic Press, New York, 1999).
- [2] M. Nolan, E. Fernandez-Grande, J. Brunskog and C.-H. Jeong, "A wavenumber approach to quantifying the isotropy of the sound field in reverberant spaces," *J. Acoust. Soc. Am.*, **143**, 2514–2526 (2018).
- [3] M. Nolan, "Estimation of angle-dependent absorption coefficients from spatially distributed in situ measurements," *J. Acoust. Soc. Am.*, **147**, EL119–EL124 (2020).
- [4] T. Masumoto, Y. Yasuda, N. Inoue and T. Sakuma, "Fast calculation of far-field sound directivity based on fast multipole boundary element method," *J. Theor. Comput. Acoust.*, **28**, 1950024 (2020).
- [5] N. A. Gumerov and R. Duraiswami, *Fast Multipole Methods for the Helmholtz Equation in Three Dimensions* (Elsevier, Oxford, 2005).
- [6] N. Nishimura, "Fast multipole accelerated boundary integral equation methods," *Appl. Mech. Rev.*, **55**, 299–324 (2002).
- [7] T. Masumoto, N. Inoue, Y. Yasuda and T. Sakuma, "Basic study on incidence directivity analysis based on FMBEM," *Proc. Autumn Meet. Acoust. Soc. Jpn.*, pp. 473–474 (2020) (in Japanese).